International Journal of Applied Pharmaceutics

ISSN- 0975-7058 Vol 18, Issue 2, 2026

Original Article

PREPARATION AND CHARACTERIZATION OF KETOPROFEN MENTHOSOME GEL AS A TOPICAL DELIVERY NANOCARRIER: EX VIVO ASSESSMENT

SAMARA MOHAMMED JASIM[1*], ABEER H. KHASRAGHI[2]

[1]Ministry of Health, Babil Health Directorate, Al Zahraa Hospital, Babil, Iraq. [2]Department of Pharmaceutics, College of Pharmacy, University of Baghdad, Baghdad, Iraq

[*]Corresponding author: Samara Mohammed Jasim; [*]Email: samara.jassem2200@copharm.uobaghdad.edu.iq

Received: 30 Sep 2025, Revised and Accepted: 29 Dec 2025

ABSTRACT

Objective: This study aimed to enhance the transdermal permeation of ketoprofen (KTP) by formulating a menthosomal gel as a vesicular nanocarrier.

Methods: KTP-loaded menthosomes were produced using the ethanol injection-probe sonication method. A mixed-level factorial design was employed to statistically investigate the effects of menthol (X_1), Span60® (X_2), and soybean lecithin (SL) (X_3) as independent variables at different actual levels on the dependent responses, including particle size (PS), polydispersity index (PDI), and entrapment efficiency (%EE). These independent variables generated fifteen experimental runs. Fourier Transform Infrared Spectroscopy (FTIR) analysis confirmed the compatibility between KTP and the excipients. The surface morphology of the menthosome was examined using Field Emission Scanning Electron Microscopy (FESEM). The selected formula was incorporated into a Carbopol 934 gel. Viscosity, pH, drug content (DC), and ex vivo permeation were used to characterize the KTP menthosomal gel.

Results: Among the formulations, K11 showed a PS of 218.4±12 nm, a PDI of 0.14±0.04, a zeta potential (ZP) of −35±2 mV, indicating high stability of the formulation, an EE% of 89.3±1.3%, and a percentage of release of 95.7±0.9% within 6 h. The FESEM images demonstrated that the KTP-loaded menthosomes exhibited a spherical morphology with a uniform distribution. KTP-excipient compatibility was confirmed by FTIR analysis. The best formula was incorporated into a gel based on Carbopol 934, which demonstrated a pH of 6±0.2, meeting the benchmark pH for skin application, and a DC of 98.7±0.8%, which is crucial for ensuring therapeutic efficacy, and an ex vivo permeation rate of 81.2±3.1% over 14 h.

Conclusion: The findings suggest that KTP-loaded menthosomes could be a promising carrier for the transdermal delivery of the hydrophobic drug; by facilitating deeper penetration and sustained delivery, these improvements can be attributed to the synergistic action of menthol with lipid-based nanocarriers. This lipoidal vesicular system effectively enhances therapeutic performance.

Keywords: Cholesterol, Ethanol injection, Franz cell, Lipid-based nanocarrier, Menthol

DOI: https://dx.doi.org/10.22159/ijap.2026v18i2.57045 Journal homepage: https://innovareacademics.in/journals/index.php/ijap

INTRODUCTION

Transdermal drug delivery offers a noninvasive approach that helps avoid factors that can affect oral drug absorption, such as stomach pH, food consumption, and gastrointestinal movement [1]. The skin has become a well-known place to administer drugs both topically and systemically in the last few decades. Compared to the oral route, transdermal delivery has several benefits. Mainly, it's used when the drug has a significant first-pass effect [2]. Further, it helps overcome issues related to poor absorption in the digestive system. Therefore, when a steady therapeutic effect is required, delivering the drug through the skin proves to be a good option [3]. Ketoprofen (KTP), a type of propionic acid derivative, is commonly used for its anti-inflammatory, pain-relieving, and fever-reducing effects. It's often prescribed to manage mild to moderate pain, including discomfort associated with menstrual cramps and rheumatoid arthritis [4]. Based on the Biopharmaceutics Classification System (BCS), KTP falls under Class II, meaning its absorption is limited by its rate of dissolution. Due to its low solubility in water, KTP is poorly absorbed in the body, leading to reduced bioavailability [5]. In addition to absorption challenges, oral forms of KTP can irritate the gastrointestinal lining, potentially causing ulcers or bleeding. Applying non-steroidal anti-inflammatory drugs (NSAIDs) like KTP topically allows the drug to act directly at the site of inflammation, which not only enhances local therapeutic effects but also minimizes gastrointestinal irritation and systemic side effects [6].

While topical delivery systems (TDSs) offer several advantages, conventional methods often struggle to penetrate the deeper layers of the skin effectively. To overcome this limitation and enhance localized drug action, vesicular drug delivery systems (VDDSs) such as niosomes and liposomes have been explored [7]. However, their relatively rigid structures limit their ability to reach deeper skin layers. In response to these challenges, researchers have developed more flexible vesicles known as elastic vesicles. These include transfersomes, which consist of lipids and edge activators, and ethosomes, which are composed of lipids combined with ethanol [8]. These systems help minimize drug loss into the bloodstream, a common issue associated with topical drug delivery methods that rely on penetration enhancers, iontophoresis, or electrophoresis. Beyond this advantage, elastic vesicles also offer the potential to bypass both the stratum corneum and the skin's capillary network, allowing the drug to be deposited in the deeper skin layers where it is most needed [9]. Transfersomes enhance their flexibility by allowing the edge activator and lipid components to reorganize within their structure, making it easier for them to pass through the skin. In contrast, ethosomes improve drug penetration by fluidizing the lipids in both the skin and the vesicles. To combine the advantages of both systems, transethosomes were developed—these specialized vesicles contain both lipids and ethanol, offering the combined properties of transfersomes and ethosomes [10]. As a consequence, the current study focuses on developing menthosomes, utilizing this established carrier system to successfully formulate a gel for the topical delivery of KTP. Menthosomes are an innovative type of ultra-deformable vesicle composed of menthol, phospholipids, an edge activator, and cholesterol. This formulation is designed to improve skin permeation and increase bilayer flexibility. The inclusion of menthol plays a critical role, as it significantly enhances transdermal drug delivery by altering the lipid bilayer structure, which boosts both drug partitioning and diffusion. When used alongside surfactants, menthol further increases skin permeability by disrupting the lipid arrangement in the stratum corneum—specifically by affecting the typical hexagonal and orthorhombic hydrocarbon chain packing. Menthol reduces the hexagonal-to-orthorhombic (RH/O) packing ratio and disturbs the tightly organized lipid matrix, leading to greater lipid fluidity within the intercellular space of the stratum corneum and facilitating more efficient drug penetration through the

skin [11]. Among the commonly used non-ionic surfactants, Span® compounds are frequently selected. In this study, Span® 60 was preferred over Span® 20 and Span® 40 due to its lower hydrophilic-lipophilic balance (HLB = 4.7), which supports the formation of stable vesicular systems. Its long, saturated alkyl chain and high phase transition temperature contribute to improved vesicle stability and drug entrapment efficiency. These properties indicate that increasing hydrophobicity helps produce more stable menthosomes with enhanced entrapment capacity [12].

MATERIALS AND METHODS

Materials

KTP was purchased from Macklin Biochemical Co., Ltd. Soybean Lecithin (SL) was purchased from Shaanxi Dideu Medichem Co, Ltd. Span®60 was obtained from Loba Chemie Pvt., India; menthol was sourced from HiMedia Laboratories Pvt. Ltd.; cholesterol was purchased from Bide Pharmatech Co., China; Carbopol 934 was procured from Alpha Chemika, India; and propylene glycol was purchased from Thomas Baker, India. A dialysis bag (MWCO 14 kDa) was purchased from Special Product Laboratory, USA.

Methods

Preparation of KTP-loaded menthosomes

KTP-loaded menthosomes were prepared using the hot method [13]. This method involves two phases: an aqueous phase and an organic phase. The two phases were prepared separately in two opaque glass containers. In summary, KTP, Span®60, cholesterol, and menthol were weighed and then dissolved in preheated 3 ml ethanol at 40 °C to form the organic phase. This solution was then dripped into 10 ml of deionized water containing SL (aqueous phase), also preheated to 40 °C, at a controlled drip rate of 1 ml/min using a syringe with a 22G needle, with continuous stirring using a magnetic stirrer/hot plate (Witeg Labortechnik GmbH, Seoul, Korea distribution partner) at 500 rpm for 1 h to ensure all ethanol molecules evaporated completely and allowed to rest until cooled down to room temperature before further vesicle size reduction by a probe sonicator (500 Watt, 20 kHz, Qsonica, 53 Church Hill Rd, Newtown, CT, USA). Vesicles formed when SL molecules dispersed in aqueous solution self-assembled into spherical bilayer shapes [14]. Finally, the dispersion was exposed to ultrasonic probe sonication for 5 min (50 seconds on, 10 seconds off with 30% amplitude) to achieve a fine-tuned dispersion with a smaller particle size [15]. The KTP-loaded menthosomes were formulated using equal quantities (100 mg) of KTP and cholesterol.

Computer-based experimental design

In this study, a mixed-level factorial design was employed to investigate the effects of menthol (X_1), Span60® (X_2), and SL (X_3) concentrations on the formulation parameters of KTP-loaded menthosomes. Each independent variable was investigated at different actual levels, as shown in table 1A [16]. The corresponding dependent responses were evaluated, including particle size (PS), polydispersity index (PDI), and entrapment efficiency (%EE), as shown in table 1B. These independent variables generated fifteen experimental runs, as shown in table 2.

The relationship between the independent variables and each response was modeled using appropriate linear polynomial regression models, as indicated by the Fit Summary. According to the model selection results, the linear polynomial model was identified as the statistically adequate model for the responses and was therefore used to describe the effect of the factors on PS, PDI, and %EE, which was expressed by the following equation (1):

$$Y = b_0 + b_1X_1 + b_2X_2 + b_3X_3$$

where Y represents the predicted response (PS, PDI, or %EE); b_0 is the intercept; b_1, b_2, and b_3 are the linear coefficients.

Table 1A: Independent variables and their corresponding experiment levels

Independent variables	Code	Number of levels	Actual level (mg)
Menthol	X_1	3	0, 100, 300
Span60®	X_2	3	100, 150, 200
SL	X_3	4	100, 150, 200, 300

Table 1B: Dependent variables and their corresponding experiment levels

Dependent variables	Code	Their levels
PS (nm)	R_1	Minimum
PDI	R_2	Minimum
%EE	R_3	Maximum

Preparation of KTP menthosomal gel

The gelling agent Carbopol 934 (1% w/v) was accurately weighed and dispersed in deionized water (8 ml) with continuous stirring for 1 h at 800 rpm to remove all air bubbles [17], before adding 2 ml of propylene glycol (as a preservative) and neutralizing it with triethanolamine [18].

Characterization study of prepared KTP-loaded menthosomes

PS, PDI, and %EE

The average PS and PDI of the prepared menthosomes were measured by dynamic light scattering (DLS) at 25 °C in a Zeta sizer Ultrared label (Malvern Instruments Ltd., Worcestershire, UK) by using a quartz cuvette [19]. From each menthosome formula (0.5 ml) diluted up to 10 ml with deionized water to ensure good sample clarity and reduce multiple scattering impact. Each sample was analyzed in triplicate [20]. The %EE refers to the proportion of the drug successfully encapsulated within the formulation. EE% was evaluated using an indirect method. To separate the free, unencapsulated KTP from the menthosomal vesicles, 1 ml of each menthosome formula was put in an Eppendorf tube and centrifuged at 14,000 rpm for 30 min at 4 °C using a cooling centrifuge (HERMLE Benchmark refrigerated microcentrifuge, Germany); the resulting supernatant was collected and diluted with ethanol. The absorbance of unentrapped KTP in the supernatant was then measured using a UV/VIS spectrophotometer at λmax 254 nm, and the corresponding concentration using a calibration curve (y = 0.0712x+0.0168, R^2 = 0.9992) [21]. EE% of the indirect method is calculated using the following equation (2):

$$EE\% = \frac{\text{Total drug} - \text{Unentrapped drug}}{\text{Total drug}} \times 100$$

In vitro dissolution studies

Before carrying out the *in vitro* dissolution study, the saturation solubility of KTP must be determined using the shake flask method. An excess amount of KTP was placed in a stoppered conical flask containing 10 ml of phosphate buffer (pH 7.4), which was shaken for 24 h at 37±0.5 °C to calculate the sink conditions and validated the dissolution medium [22]. This study was carried out using a USP dissolution test apparatus II (paddle method) at a stirring speed of 50 rpm and 500 ml of pH 7.4 phosphate buffer for 6 h at 37±0.5 °C as the dissolution medium [23]. Drug release from KTP-loaded men-

thosomal formulations was investigated by the dialysis bag procedure (MWCO 14 kDa) [24]. Prior to conducting the experiment, the dialysis membrane was pretreated by soaking in phosphate buffer solution (PBS, pH 7.4) for 24 h [25]. One ml of KTP-loaded menthosome formulation (equivalent to 10 mg KTP) was placed in the dialysis membrane. Samples of 5 ml were taken after specific time intervals (0.08, 0.16, 0.25, 0.33, 0.5, 0.75, 1, 1.5, 2, 2.5, 3, 4, 5, 6 h) and replaced with fresh phosphate buffer [26]. The samples were then filtered and analyzed by UV/VIS spectrophotometry (Shimadzu, model UV-1601 PC, Kyoto, Japan) at λmax 260 nm [27], and the corresponding concentration was determined using a calibration curve (y = 0.0658x+0.0123, R^2 = 0.9995) to construct the release profile of the KTP menthosome formulations [28].

Release kinetics of KTP-loaded menthosomes

To elucidate the mechanism of KTP release from the prepared menthosome formulations, the *in vitro* release data (up to 6 h) were fitted to various kinetic models: zero-order, first-order, Higuchi, and Korsmeyer-Peppas. The best-fitting model was chosen depending on the models' highest correlation coefficients (R^2). The *n* value is the KTP release exponential that characterizes the drug release mechanism. When the *n* value *is* less than 0.43, there is a Fickian diffusion mechanism and a non-swellable matrix diffusion release mechanism; when *the n* value is more than 0.43, there is anomalous transport (both diffusion and erosion) [29].

Field emission scanning electron microscopy (FESEM)

The morphology of the selected formula (K11) was examined using FESEM; this analysis provided insights into key characteristics such as PS, shape, and surface texture [30].

Fourier-transform infrared spectroscopy (FTIR)

To assess the compatibility and ensure no interactions occurred between the components used in formulating the KTP-loaded menthosomes, an FTIR analysis was carried out [31]. The FTIR spectra were recorded using a Shimadzu FTIR-43000 spectrometer (Japan). Each sample was carefully mixed with potassium bromide (KBr) and compressed into clear discs. Spectral data were collected over the range of 4000–400 cm^{-1} with a resolution of 4 cm^{-1} [32].

Zeta potential (ZP)

The Zeta Sizer Ultra (red label) (Malvern Instruments Ltd., Worcestershire, UK) measures the intensity and charge type of the menthosomal vesicle surface based on electric mobility at 25 °C. Only the selected formula (K11) was subjected to ZP measurements. Measurements were carried out in triplicate, and results were expressed as the mean ZP (mV) [15].

Characterization study of the prepared KTP menthosomal gel

Measurement of pH

The pH of KTP menthosomal gel was determined using a digital pH meter at room temperature. Ensuring the pH of the gel is compatible with skin pH is important to minimize the risk of skin irritation [33]. One g of the KTP menthosomal gel was dispersed into 100 ml of deionized water and sonicated for 5 min [34]. The pH meter requires calibration prior to each single use [35].

Measurement of drug content (DC)

An exact amount of 0.2 g of the selected KTP menthosomal gel (theoretically equivalent to 2 mg of KTP) was weighed and dissolved in ethanol up to 10 ml. The resulting solution was investigated by a UV/VIS spectrophotometer at λmax = 254 to calculate the DC after dilution with the proper volume of ethanol [36]. The % DC in the KTP menthosomal gel was determined using the following equation (3).

$$\text{Drug content \%} = \frac{\text{Measured amount of KTP}}{\text{Theoretical amount of KTP}} \times 100$$

Measurement of viscosity

The viscometer was calibrated correctly to obtain dependable and accurate readings. The viscosity was measured at room temperature using a viscometer (Myr VR3000, Visotech, Spain). The rotation speed was gradually increased from 0 to 200 with the spindle no. 7 (R7) [37].

Ex-vivo permeation study

An ex vivo skin permeation study was performed using a Franz diffusion cell (had a diffusion area of 3.14 cm^2 and a 25 ml volume capacity) [25]. Approval and prior authorization were obtained from the Research Ethics Committee under project number (REC032435R). Male Wistar Albino rats (weighing 150±25 g) were used in this study; the abdominal side of the rat hair was shaved carefully, followed by the extraction of its connective tissue and subcutaneous fat, and used freshly. Between the donor and receptor compartments, the excised skin of the rat was placed, with the stratum corneum facing towards the donor compartment [38]. A permeation study was performed using a KTP menthosomal gel, Fastum® gel, and KTP plain gel. One g of the KTP menthosomal gel, KTP plain gel, and 0.4 g of the Fastum® gel (dispenser tube of 50 g), which is equivalent to 10 mg of the KTP, were placed on the stratum corneum of the skin specimen. The receptor compartment was filled with phosphate buffer (pH 7.4), which was maintained at 37±0.5 °C and magnetically stirred at 300 rpm. The samples were collected (2 ml) at specific time points (1, 2, 4, 6, 8, 10, 12, and 14 h) [28], replaced with an equal volume of pH 7.4 buffer to maintain the sink conditions, and analyzed by UV/VIS spectrophotometry at 260 nm [39].

Statistical analysis

The experimental data were analyzed using Design-Expert® version 13.0.5.0 software. The relationship between the independent variables and the observed responses was modeled using appropriate regression models (primarily linear polynomial models as indicated by the fit summary). Model adequacy and the significance of individual terms were evaluated using analysis of variance (ANOVA). All model terms were considered statistically significant at $P<0.05$. The results were summarized as mean±standard deviation (SD) for three samples (in triplicate, n = 3). To compare the differences between group means where applicable, a one-way ANOVA followed by Tukey's post hoc test was performed, and statistical significance was set at $P<0.05$.

RESULTS AND DISCUSSION

Evaluation of the KTP-loaded menthosomes

The main drawbacks of the thin film hydration method were the production of menthosomes with low %EE and the fact that the technique required more time. In contrast, the ethanol injection method offers several advantages, including simplicity, a faster technique, and the use of ethanol as a safe solvent, as well as a higher %EE [40].

PS, PDI, and %EE

The PS of KTP-loaded menthosomes varied within the range of 152.8±36 to 786.5±40 nm, the PDI values were observed in the range of 0.068±0.010 to 0.228±0.049, and the %EE of KTP-loaded menthosomes ranged from 15.9±3% to 89.3±1.3%, as shown in table 2.

Model terms with a p-value less than 0.0500 were considered significant, whereas those with values above 0.1000 were regarded as insignificant.

As shown in table 3, the PS model was statistically significant, as indicated by an F-value of 9.8, with p-value 0.006. For PS, the factors identified as significant included A. The model for PDI model was statistically insignificant, as evidenced by an F-value of 1.15 with p-value 0.37. The EE% model was found to be statistically significant, with an F-value of 18.9, with p-value 0.001. Among the evaluated variables, factor A exhibited the strongest influence, as indicated by an F-value of 96.3.

As presented in table 2, increasing the concentration of menthol resulted in a reduction of PS, because menthol acts as an edge activator. This effect can be attributed to menthol's ability to improve lipid fluidity within the stratum corneum and to disturb the tightly

packed hexagonal and orthorhombic hydrocarbon chain arrangements, thereby loosening the lipid packing; similar findings have been reported by Nayak D *et al.* [41]. PDI serves as an indicator of the homogeneity of a formulation. Value closer to 0 denote a monodisperse distribution, while those approaching 1 reflect a broad and heterogeneous vesicle population. The PDI of the formulations was within the range (0.068 to 0.228), indicating that the menthosome formulations prepared were homogenous; Al-Sawaf *et al.*'s study noted similar results [15]. Increasing the concentration of menthol resulted in a decrease in EE%. While menthol enhances bilayer elasticity and flexibility, its rising concentration introduces competition with KTP, which is hydrophobic and preferentially localizes within the lipid domains. This competition limits the available space within the bilayer for drug incorporation, thereby reducing the overall %EE [41]. Additionally, the presence of non-ionic surfactant (Span® 60) and SL contributes to encapsulation, enabling the drug to partition into both the lipid bilayer and the aqueous core of the vesicles; similar effects have been reported by Manjushree *et al.* [42].

Table 2: Mixed-level factorial design matrix and the observed experimental responses

Run	Factor 1 X_1 menthol (mg)	Factor 2 X_2 Span®60 (mg)	Factor 3 X_3 SL (mg)	Response 1 R_1 PS (nm)	Response 2 R_2 PDI	Response 3 R_3 %EE
k1	0	200	100	578.2±65	0.138±0.061	78.6±2.6
k2	100	200	100	382.7±12	0.101±0.030	81.7±1.5
k3	300	200	100	215±41	0.133±0.035	15.9±3
k4	0	100	200	415.5±32	0.16±0.051	74.4±2
k5	100	100	200	267.5±29	0.111±0.029	78.9±2
k6	300	100	200	213.3±21	0.068±0.010	30.9±3.6
K7	0	150	150	658.7±72	0.228±0.049	76.6±3
K8	100	150	150	268±51	0.196±0.133	82.3±2.1
K9	300	150	150	152.8±36	0.155±0.035	35.5±6.3
K10	0	100	300	447±32	0.170±0.048	76.8±2.2
K11	100	100	300	218.4±12	0.141±0.040	89.3±1.3
K12	300	100	300	165.5±28	0.145±0.038	25.2±6.3
K13	0	200	300	786.5±40	0.102±0.085	62.2±3.8
K14	100	200	300	299.6±35	0.131±0.058	67.5±2.4
K15	300	200	300	210±41	0.099±0.082	33.4±5.1

The results were expressed as mean±SD (n = 3)

Table 3: Summary of statistical models with F value and p-value of corresponding responses

Source	PS		PDI		% EE	
	F-value	p-value	F-value	p-value	F-value	p-value
Model	9.08	0.0026	1.15	0.3727	12.24	0.0008
A	23.66	0.0005	2.25	0.1614	35.88	0.0001
B	3.35	0.0942	0.76	0.4012	0.76	0.3993
C	0.040	0.8440	0.76	0.4015	0.22	0.6453

A: Menthol, B: Span 60, C: Soybean lecithin

In vitro drug release study

The saturation solubility value of KTP in phosphate buffer (pH 7.4) was found to be 8.12±1.3 mg/ml. *In vitro* drug release was carried out only for formulas with the highest %EE (K11, K8) and free drug. During the 6 h release assay, the drug was released from the menthosomal vesicles. All the vesicular delivery systems demonstrated an ability to control the release of the drug [43]. Formulations with the highest %EE, K11, showed a higher release percentage (95.7±0.9%) compared to formulation K8 (%EE of 87±2.1%) [44]. Although both K11 and K8 had relatively high % EE values, the superior release from K11 can be attributed to its higher concentration of SL, which acts as a penetration enhancer [45].

As shown in fig. 1B, the *in vitro* drug release model demonstrated strong statistical significance, reflected by an F-value of 555 (****P<0.0001).

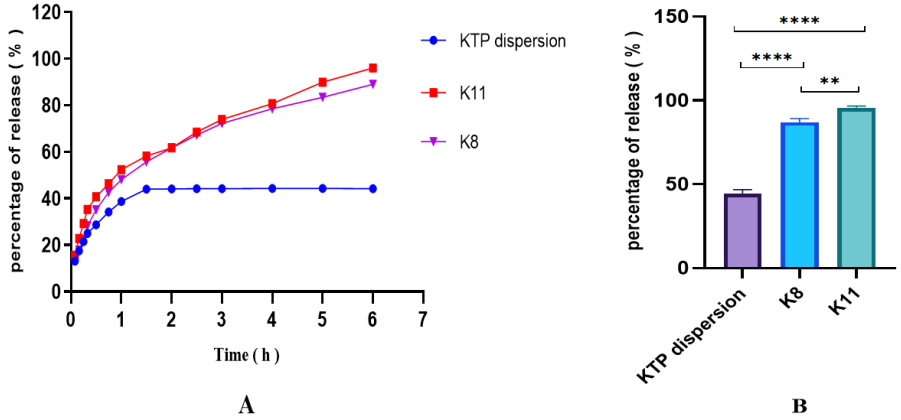

Fig. 1: A-*In vitro* dissolution profile of pure KTP, K11, and K8, B-Statistical comparison analysis of *in vitro* release of pure KTP, K11, and K8, mean±SD (n=3). One-way ANOVA followed by Tukey's multiple comparison test showed highly significant differences between pure KTP and K8 (**p<0.0001) and between pure KTP and K11 (****p<0.0001), as well as a significant difference between K8 and K11 (**p = 0.0047), The calculated correlation coefficients (R^2), release constants (K), and release exponent (n) are presented in table 4**

Table 4: Summary of KTP release kinetic modeling for the formulations K8 and K11

Formula	Zero order		First order		Higuchi model		Korsmeyer Peppas model		
	K_0	R^2	K_1	R^2	K_H	R^2	K_{KP}	*N*	R^2
K8	0.335	0.2134	0.009	0.8846	5.280	0.9525	6.279	0.491	0.9948
K11	0.369	0.0195	0.012	0.8923	5.858	0.9181	8.752	0.441	0.9890

K_0: Zero order release constant, K_1: First order release constant, K_H: Higuchi release constant, K_{KP}: Korsmeyer-Peppas release constant, R^2: correlation coefficient, n: release exponent

As shown in table 4, the Korsmeyer-Peppas model exhibited the highest R^2 values for both formulations (K8: R^2 = 0.9948; K11: R^2 = 0.9890), indicating it was the best-fit model. To further understand the release mechanism, the release exponent '*n*' was evaluated. The '*n*' values for formulations K8 and K11 were 0.491 and 0.441, respectively. Since both values were more than 0.43, this suggests that the KTP release mechanism from the menthosome formulations is predominantly governed by non-Fickian diffusion and erosion.

Determining the selected formula

To complete the remaining tests, select the best formulation, which exhibits a PS (218.4±12 nm), a PDI (0.14±0.04), the highest %EE (89.3±1.3%), and the highest % of release (95.7±0.9%) over 6 h. As a result, the formula K11 from table 2 was chosen.

FESEM

The morphological aspects of the selected KTP-loaded menthosome formulation were investigated using FESEM. Fig. 2 revealed FESEM images in different nanoscale sizes. The FESEM images demonstrated that the KTP-loaded menthosomes exhibited a roughly spherical morphology with a uniform distribution [46]. However, the PS measured by DLS was larger than that observed in the FESEM images. This discrepancy is expected, as DLS measures the hydrodynamic diameter, which includes layers of water surrounding the menthosomes, resulting in larger sizes in solution, whereas FESEM analysis was conducted on dry particles [47]. DLS intensity-based distributions are inherently more sensitive and biased towards larger particle populations. However, the formulation's low PDI of 0.14 signifies a relatively monodisperse system, a finding that corroborates the uniform particle morphology observed in the FESEM images.

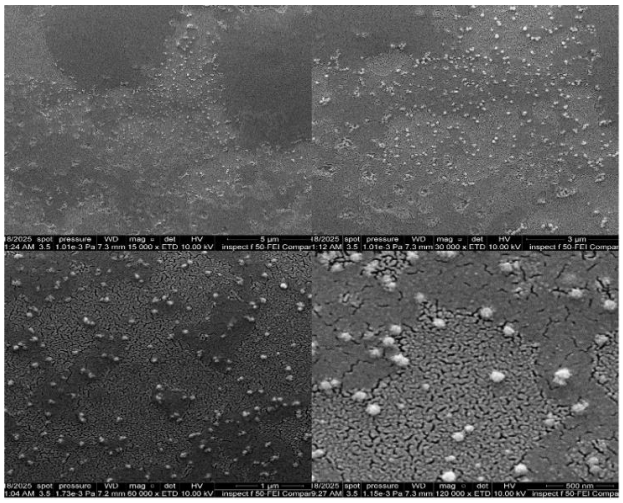

Fig. 2: FESEM image of the K11 formula showing menthosome vesicles in the nanometer range

ZP determination

ZP is an essential parameter for assessing the stability of colloidal dispersions through both physical and chemical mechanisms. Physically, it represents the electrostatic potential at the interface between dispersed particles and their surrounding medium. Higher ZP values are generally associated with improved stability, as strong repulsive forces prevent particle aggregation. Conversely, lower ZP values indicate weaker repulsion, allowing attractive forces to dominate and promoting particle clustering [48]. Chemically, the anionic environment may protect the unsaturated lipids in SL component from oxidative degradation, thereby contributing to long-term stability of the system [49]. Fig. 3 shows a ZP of selected KTP-loaded menthosome formula (K11) of-35±2 mV, indicating high stability of the formulation. A possible source for the negative charge on the surface of the menthosome vesicles is the presence of anionic phosphate groups ($-PO_4^{2-}$) in the phospholipid contributed to the formula [50]. The presence of cholesterol, which plays a key role in enhancing colloidal stability by reducing the likelihood of vesicle fusion or particle aggregation during storage [51].

FTIR

The FTIR spectra exhibit distinct peaks of pure KTP and other components in the menthosome formulation.

For pure KTP, it showed the drug's unique "fingerprints," especially the two strong carbonyl (C=O) peaks at 1695 cm^{-1} (from the carboxylic acid) and 1653 cm^{-1} (from the ketone). We also noted its other key features, like the broad O–H stretch around 3417 cm^{-1} and the aliphatic C–H stretches (2976-2935 cm^{-1}).

When we analyzed the simple physical mixture (PM), the spectrum was essentially a straightforward composite of all the individual ingredients. The two critical KTP C=O signals were still clearly visible at 1697 cm^{-1} and 1653 cm^{-1}. This was a crucial finding, as it confirmed that no strong chemical reactions occurred just from mixing, validating the components' compatibility.

In sharp contrast, the spectrum for the final K11 formulation told a completely different and more significant story. It provided definitive proof of drug encapsulation. The two distinct C=O peaks that define crystalline KTP had disappeared. In their place, a new, strong, and slightly broader band emerged at 1637 cm^{-1}.

This dramatic shift shows that the KTP's natural intermolecular hydrogen bonding (its dimer structure) was disrupted. Instead, the drug's functional groups (C=O and O-H) formed new hydrogen-bonding interactions with the excipient molecules (such as the phospholipid's P=O and the O-H groups from cholesterol and menthol).

This confirms that the KTP was no longer present in its original crystalline form but was successfully entrapped and molecularly dispersed within the lipid-menthol matrix of the menthosome [38].

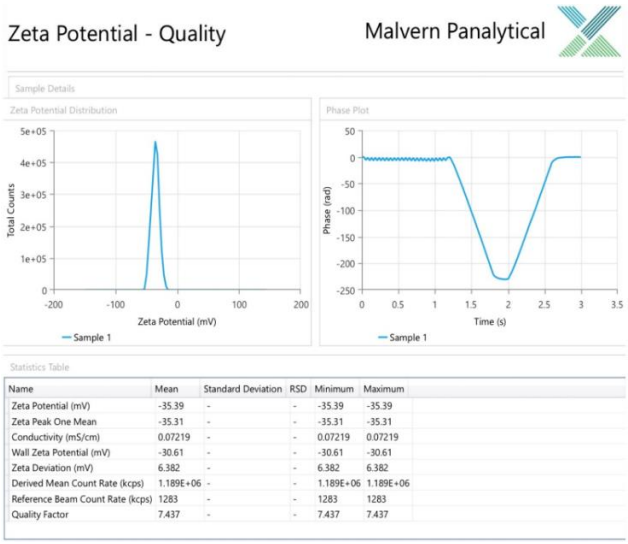

Name	Mean	Standard Deviation	RSD	Minimum	Maximum
Zeta Potential (mV)	-35.39	-	-	-35.39	-35.39
Zeta Peak One Mean	-35.31	-	-	-35.31	-35.31
Conductivity (mS/cm)	0.07219	-	-	0.07219	0.07219
Wall Zeta Potential (mV)	-30.61	-	-	-30.61	-30.61
Zeta Deviation (mV)	6.382	-	-	6.382	6.382
Derived Mean Count Rate (kcps)	1.189E+06	-	-	1.189E+06	1.189E+06
Reference Beam Count Rate (kcps)	1283	-	-	1283	1283
Quality Factor	7.437	-	-	7.437	7.437

Fig. 3: Zeta potential and surface charge analysis of the K11 formula evaluating stability

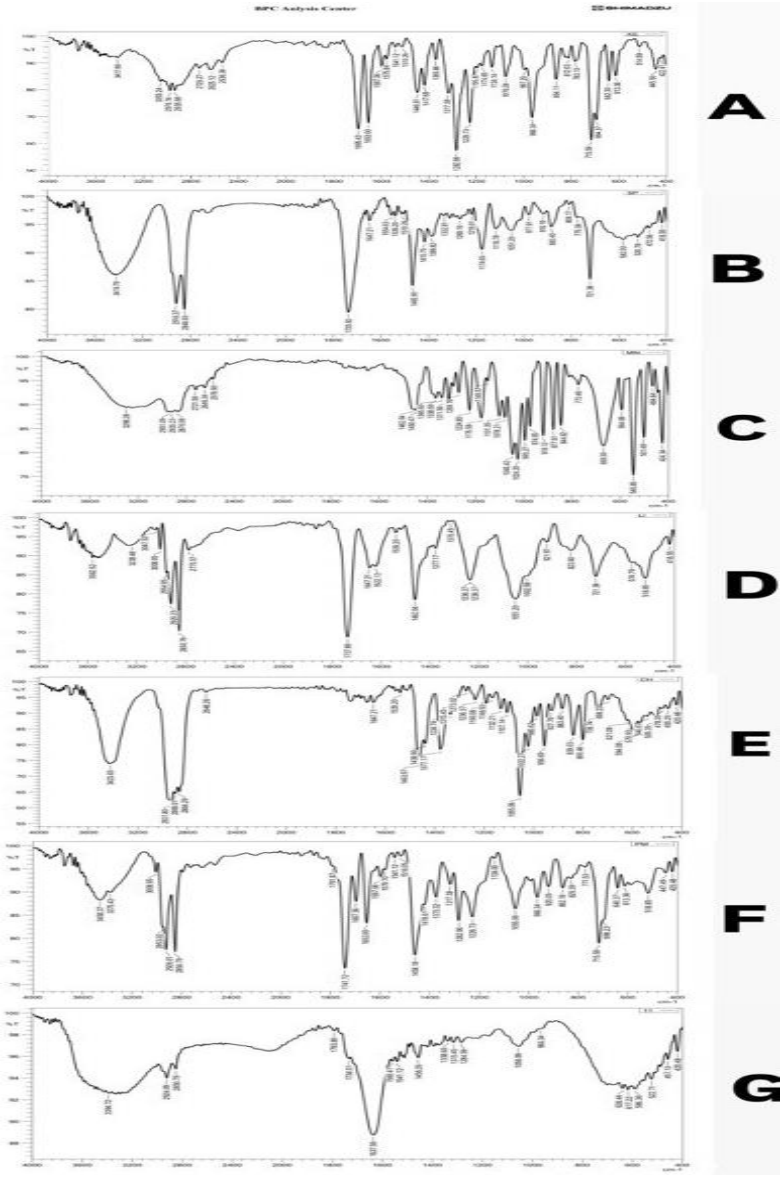

Fig. 4: FTIR of pure KTP, Span® 60, Menthol, SL, Cholesterol, PM (Physical mixture), and K11 (A, B, C, D, E, F and G), respectively, showing drug-excipient compatibility

Evaluation of the prepared KTP menthosomal gel

Determination of pH

The KTP menthosomal gel showed a pH of 6±0.2, meeting the benchmark pH for skin application to minimize the risk of skin irritation, which is particularly important for formulations intended for sensitive skin [52].

Determination of DC

The %DC for the KTP menthosomal gel was 98.7±0.8%, referring to a high level of accuracy in the preparation method (the drug was efficiently incorporated within the formulation and uniformly distributed within the gel), which is crucial for ensuring therapeutic efficacy.

Determination of the viscosity

The KTP menthosomal gel showed a shear-thinning profile, where viscosity declined as the shear rate increased, which was advantageous because it enhanced spreadability during application on skin [53].

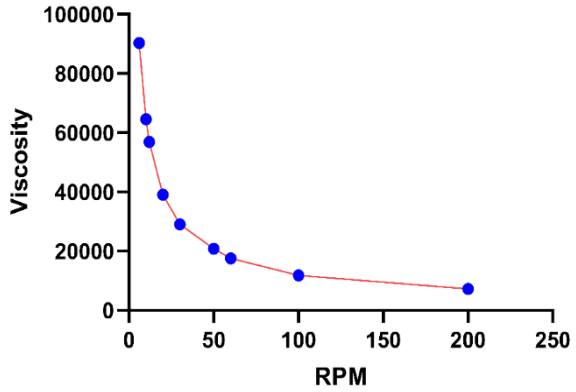

Fig. 5: Viscosity profile of the KTP menthosomal gel

Ex vivo permeation study

Transdermal permeation measurement of a drug is a critical step in formulation development. An ex vivo skin permeation study was performed on the KTP menthosomal gel, Fastum® gel, and KTP plain gel. The results showed that the KTP menthosomal gel achieved a permeation of 81.2±3.1% at 14 h, compared with 63.4±4.6% for Fastum® gel and 33.7±5.2% for KTP plain gel (fig. 6A).

Ex vivo permeation was carried out only on the selected KTP menthosomal gel based on the K11 formulation because it demonstrated a significantly higher *in vitro* drug release percentage (**p<0.01) compared with pure KTP and another formulation (K8). At 6 h, the percentage of permeated drug from the selected KTP menthosomal gel was 53.8%, which was lower than the *in vitro* drug release of the same formulation (95.7%). This reduction may be attributed to slow diffusion of the drug, first from the menthosomal vesicles, followed by delayed diffusion from the gel matrix (gel viscosity effect), as well as the difference in thickness of rat skin compared with the dialysis membrane [54]. Previous studies have shown similar findings with other drug-loaded menthosomes. For example, a study by Nayak D *et al.* (2024) found that ex vivo skin permeation of the optimized menthosome formulation of ibuprofen exhibited a drug release of 60.05±2.80% over 7.5 h, significantly higher than the conventional liposome, which had a drug release of 15.42±1.97% [41]. Another study by Manjushree H *et al.* (2025) on ketoconazole-loaded menthosomes reported a cumulative drug permeation of the optimized formulation reached 67.70±0.64%; in contrast, the marketed formulation was observed at 45.42±1.03%, and conventional liposomes were observed at 55.3±0.86% [42], indicating that menthosome formulations generally exhibit higher skin permeation compared to traditional nanocarrier systems.

Fig. 6B illustrated a significant enhancement of KTP permeation (****p<0.0001) from the menthosomal gel compared with KTP plain gel due to vesicular components, which increased flexibility and fluidity by redistributing the penetration enhancer (Span® 60), menthol, cholesterol, and SL through the stratum corneum of the rat skin [55], and (**p<0.01) from Fastum® gel because menthol is thought to disrupt the ceramide-based hydrogen bonding network within skin lipid bilayers [56]. When skin is treated with menthol, alterations in the epidermal structure, along with the formation of microcavities, are observed. These microcavities may act as drug reservoirs, supporting sustained release and facilitating diffusion [57].

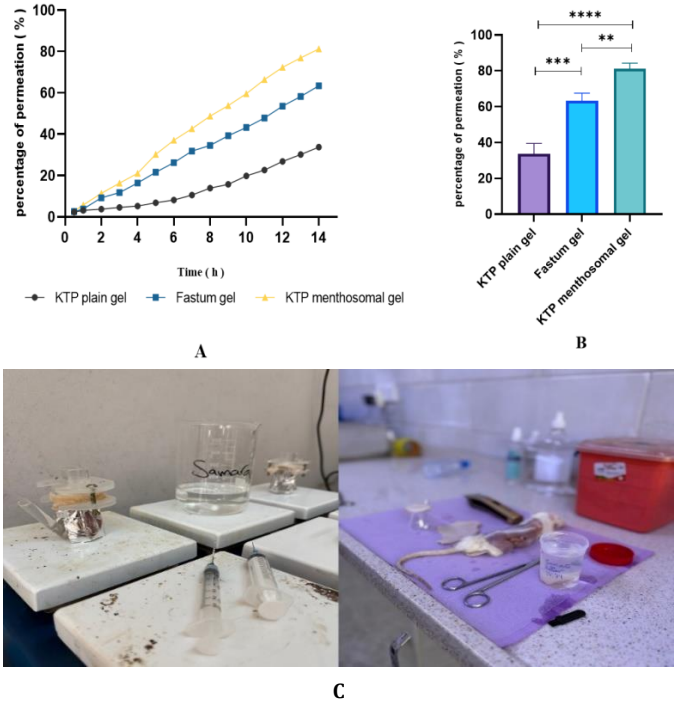

Fig. 6: A-Ex vivo skin permeation profile of KTP menthosomal gel, Fastum® gel, and KTP plain gel, B-Statistical comparison analysis of ex vivo permeation of KTP menthosomal gel, Fastum® gel, and KTP plain gel mean±SD (n=3). One-way ANOVA with Tukey's post-hoc test showed significant differences between KTP plain gel and KTP menthosomal gel (**p<0.0001), KTP plain gel and Fastum® gel (****p = 0.0001), and Fastum® gel and KTP menthosomal gel (**p = 0.0067), C-Experimental setup of the Franz diffusion cell for ex vivo skin permeation study.**

CONCLUSION

The study successfully developed KTP-loaded menthosomes using the ethanol injection–probe sonication technique. The optimized formulation demonstrated favorable characteristics, including suitable PS, narrow PDI, stable ZP, high %EE, and an *in vitro* release exceeding 90% within 6 h. Furthermore, ex vivo skin permeation experiments confirmed significantly improved drug permeation compared to the plain gel. These improvements can be attributed to the synergistic action of menthol with lipid-based nanocarriers. By facilitating deeper penetration and sustained delivery, this lipoidal vesicular system effectively enhances therapeutic performance. Overall, the results indicate that KTP-loaded menthosomes represent a promising platform for the transdermal delivery of hydrophobic drugs.

However, a limitation of the current study is the lack of a short-term stability evaluation of the optimized menthosomal dispersion (K11) and the final gel. Assessing changes in key parameters such as PS, PDI, ZP, and %EE over time (e. g., 1–3 mo at 4 °C and 25 °C) would provide valuable insights into the formulation's shelf life and robustness. Therefore, conducting comprehensive stability studies should be considered a key objective for future research to further validate the practical applicability of this promising delivery system.

ACKNOWLEDGEMENT

The authors gratefully acknowledge the Department of Pharmaceutics, College of Pharmacy, University of Baghdad, for their valuable support throughout this study.

FUNDING

The authors received no financial support from any agencies.

ETHICS STATEMENTS

The study protocol was approved by the University of Baghdad-College of Pharmacy Research Ethics Committee under project number (REC032435R).

AUTHORS CONTRIBUTIONS

Samara Mohammed Jasim: Writing—original draft, Resources, Methodology, Formal analysis. Abeer H. Khasraghi: Writing—review and editing, validation, supervision, and conceptualization.

CONFLICT OF INTERESTS

The authors declare that they have no known competing financial interests or personal relationships that could have appeared to influence the work reported in this paper.

REFERENCES

1. Alkilani AZ, McCrudden MT, Donnelly RF. Transdermal drug delivery: innovative pharmaceutical developments based on disruption of the barrier properties of the stratum corneum. Pharmaceutics. 2015 Oct;7(4):438-70. doi: 10.3390/pharmaceutics7040438, PMID 26506371.
2. Miller MA, Pisani E. The cost of unsafe injections. Bull World Health Organ. 1999;77(10):808-11. PMID 10593028.
3. Callaghan TM, Wilhelm KP. A review of ageing and an examination of clinical methods in the assessment of ageing skin. Part 2: clinical perspectives and clinical methods in the evaluation of ageing skin. Int J Cosmet Sci. 2008 Oct;30(5):323-32. doi: 10.1111/j.1468-2494.2008.00455.x, PMID 18822037.
4. Ahmed IS, Nafadi MM, Fatahalla FA. Formulation of a fast-dissolving ketoprofen tablet using freeze-drying in blisters technique. Drug Dev Ind Pharm. 2006 Apr;32(4):437-42. doi: 10.1080/03639040500528913, PMID 16638681.
5. Abd-Elrahman AA, El Nabarawi MA, Hassan DH, Taha AA. Ketoprofen mesoporous silica nanoparticles SBA-15 hard gelatin capsules: preparation and *in vitro*/*in vivo* characterization. Drug Deliv. 2016 Nov;23(9):3387-98. doi: 10.1080/10717544.2016.1186251, PMID 27167529.
6. Ferreira LM, Cervi VF, Gehrcke M, Da Silveira EF, Azambuja JH, Braganhol E. Ketoprofen-loaded pomegranate seed oil nanoemulsion stabilized by pullulan: selective antiglioma formulation for intravenous administration. Colloids Surf B Biointerfaces. 2015 Jun;130:272-7. doi: 10.1016/j.colsurfb.2015.04.023, PMID 25935266.
7. Bhatia A, Singh B, Raza K, Wadhwa S, Katare OP. Tamoxifen-loaded lecithin organogel (LO) for topical application: development optimization and characterization. Int J Pharm. 2013 Feb;444(1-2):47-59. doi: 10.1016/j.ijpharm.2013.01.029, PMID 23353077.
8. Solanki AB, Parikh JR, Parikh RH. Formulation and optimization of piroxicam proniosomes by 3-factor, 3-level box-behnken design. AAPS PharmSciTech. 2007;8(4):E86. doi: 10.1208/pt0804086, PMID 18181547.
9. El Zaafarany GM, Awad GA, Holayel SM, Mortada ND. Role of edge activators and surface charge in developing ultradeformable vesicles with enhanced skin delivery. Int J Pharm. 2010 Sep;397(1-2):164-72. doi: 10.1016/j.ijpharm.2010.06.034, PMID 20599487.
10. Song CK, Balakrishnan P, Shim CK, Chung SJ, Chong S, Kim DD. A novel vesicular carrier transethosome for enhanced skin delivery of voriconazole: characterization and *in vitro*/*in vivo* evaluation. Colloids Surf B Biointerfaces. 2012 Apr;92:299-304. doi: 10.1016/j.colsurfb.2011.12.004, PMID 22205066.
11. Nayak D, Tippavajhala VK. A comprehensive review on preparation, evaluation and applications of deformable liposomes. Iran J Pharm Res. 2021;20(1):186-205. doi: 10.22037/ijpr.2020.112878.13997, PMID 34400952.
12. Mitrovic D, Zaklan D, Danic M, Stanimirov B, Stankov K, Al-Salami H. The pharmaceutical and pharmacological potential applications of bilosomes as nanocarriers for drug delivery. Molecules. 2025 Mar;30(5):1181. doi: 10.3390/molecules30051181, PMID 40076403.
13. Shanta Taher SS, Sadeq ZA, Al-Kinani KK, Alwan ZS. Solid lipid nanoparticles as a promising approach for delivery of anticancer agents: review article. Mil Med Sci Lett. 2022;91(3):197-207. doi: 10.31482/mmsl.2021.042.
14. Sforzi J, Palagi L, Aime S. Liposome-based bioassays. Biology (Basel). 2020;9(8):202. doi: 10.3390/biology9080202, PMID 32752243.
15. Al-Sawaf OFB, Jalal F. Novel probe sonication method for the preparation of meloxicam bilosomes for transdermal delivery: part one. J Res Med Dent Sci. 2023;11(6):5–12.
16. Khalifa NE, Nur AO, Osman ZA. Artemether-loaded ethylcellulose nanosuspensions: effects of formulation variables, physical stability and drug release profile. Int J Pharm Pharm Sci. 2017 Jun;9(6):90. doi: 10.22159/ijpps.2017v9i6.18321.
17. Gupta V, Joshi NK. Formulation development and evaluation of ketoprofen-loaded transethosomes gel. J Drug Deliv Ther. 2022 Jan;12(1):86-90. doi: 10.22270/jddt.v12i1.5177.
18. De Spiegeleer B, Wattyn E, Slegers G, Van Der Meeren P, Vlaminck K, Van Vooren L. The importance of the cosolvent propylene glycol on the antimicrobial preservative efficacy of a pharmaceutical formulation by DOE-ruggedness testing. Pharm Dev Technol. 2006 Jan;11(3):275-84. doi: 10.1080/10837450600767342, PMID 16895838.
19. Oudah SA, Al-Khedairy EB. Development and characterization of bilastine nanosuspension for enhanced dissolution in orodispersible films. Open Nano. 2025;21:100230. doi: 10.1016/j.onano.2024.100230.
20. Salih OS, Al-Akkam EJ. Preparation *in-vitro* and ex-vivo evaluation of ondansetron-loaded invasomes for transdermal delivery. IJPS. 2023;32(3):71-84. doi: 10.31351/vol32iss3pp71-84.
21. Modi C, Bharadia P. *In vitro* and ex-vivo evaluation of transfersomal gel of methotrexate. Braz J Pharm Sci. 2023;59:e22643. doi: 10.1590/s2175-97902023e22643.
22. Abbas HK, Wais FMH, Abood AN. Preparation and evaluation of ketoprofen nanosuspension using solvent evaporation technique. Iraqi J Pharm Sci. 2017;26(2):41-55. doi: 10.31351/vol26iss2pp41-55.
23. Wannas AN, Abdul-Hasan MT, Mohammed Jawad KKM, Razzaq IF. Preparation and *in vitro* evaluation of self-nanoemulsifying drug delivery systems of ketoprofen. Int J Appl Pharm. 2023 May;15(3):71-9. doi: 10.22159/ijap.2023v15i3.46892.
24. Oudah MH. Formulation and characterization of ketoprofen nanoparticles as hydrogel dosage form. Kufa J Pharm Sci. 2025;2(1):14-22.

25. Al-Mahmood S, Rajab NA. Effect of unsaturated fatty acids on the topical delivery of caspofungin ufasomes: *in vitro*/ ex vivo evaluation and anti-fungal study against Candida albicans. Open-Nano. 2025 Jul;24:100250. doi: 10.1016/j.onano.2025.100250.
26. Tous S, Fathy MF, Fetih G, Gad SF. Preparation and evaluation of ketoprofen-loaded calcium alginate beads. Int J PharmTech Res. 2014;6(3):1100–12.
27. Silalahi AA, Ramlan Sinaga K, Sumaiyah S. Formulation and evaluation of ketoprofen transdermal matrix patch containing different polymer components. Asian J Pharm Clin Res. 2018 Nov;11(11):316. doi: 10.22159/ajpcr.2018.v11i11.27282.
28. Kadam RD, Gunesh N, Dhembre, Umesh T, Jadhao, Sandip T, Thoke, Dharamraj A, Rathod, Venkatesh, R Kauthekar. Formulation and evaluation of a sustained-release matrix tablet of ketoprofen. World J Bio Pharm Health Sci. 2024;20(2):295-304. doi: 10.30574/wjbphs.2024.20.2.0875.
29. Rozas R, Ortiz AC, Penaloza S, Lizama S, Flores ME, Morales J. Kinetic and methodological insights into hydrophilic drug release from mesoporous silica nanocarriers. Pharmaceutics. 2025 May;17(6):694. doi: 10.3390/pharmaceutics17060694, PMID 40574007.
30. Muhammed SA, Al-Kinani KK. Formulation and *in vitro* evaluation of meloxicam as a self-microemulsifying drug delivery system. F1000Res. 2023 May;12:315. doi: 10.12688/f1000research.130749.2, PMID 37359788.
31. Khudhair AS, Sabri LA. Preparation and evaluation of topical hydrogel containing ketoconazole-loaded bilosomes. Acta Pharm Sci. 2024;62(4):762. doi: 10.23893/1307-2080.APS6250.
32. Ali SK, Al-Akkam EJ. Oral nanobilosomes of ropinirole: preparation compatibility and ex-vivo intestinal absorption study. J Adv Pharm Educ Res. 2023;13(4):8-15. doi: 10.51847/B7uaDLOWfq.
33. Kmkm AM, Ghareeb MM. Natural oil nanoemulsion-based gel vehicle for enhancing antifungal effect of topical luliconazole. J Fac Med Baghdad. 2023 Apr;65(1):65-73. doi: 10.32007/jfacmedbagdad.6512058.
34. Kasparaviciene G, Maslii Y, Herbina N, Kazlauskiene D, Marksa M, Bernatoniene J. Development and evaluation of two-phase gel formulations for enhanced delivery of active ingredients: sodium diclofenac and camphor. Pharmaceutics. 2024 Mar;16(3):366. doi: 10.3390/pharmaceutics16030366, PMID 38543261.
35. Ahmed MM, Fatima F, Anwer MK, Ibnouf EO, Kalam MA, Alshamsan A. Formulation and *in vitro* evaluation of topical nanosponge-based gel containing butenafine for the treatment of fungal skin infection. Saudi Pharm J. 2021 May;29(5):467-77. doi: 10.1016/j.jsps.2021.04.010, PMID 34135673.
36. Gavat CC. Ultraviolet (UV) spectrophotometric analysis of ketoprofen in tablets–statistical validation of proposed method. In: The 4th International Online Conference on Nanomaterials, Basel Switzerland: MDPI; 2023. p. 60. doi: 10.3390/IOCN2023-14442.
37. Hassan M, Sabri LA. Development and evaluation of aceclofenac-loaded nanosponge hydrogel for enhanced topical anti-inflammatory delivery. Int J Appl Pharm. 2025 Mar;17(2):104-14. doi: 10.22159/ijap.2025v17i2.53014.
38. Kar K, Sudheer P. Formulation and evaluation of niosomal drug delivery system of ketoprofen. RGUHS J PharmSci. 2016 Jan;5(4):173-80. doi: 10.5530/rjps.2015.4.7.
39. K Chandur V, TK T, Shabaraya A R. Comparative characterization of gel-loaded ketoprofen nanosponges for topical delivery. Int J Health Sci Res. 2023 Jan;13(1):44-58. doi: 10.52403/ijhsr.20230108.
40. Lombardo D, Kiselev MA. Methods of liposomes preparation: formation and control factors of versatile nanocarriers for biomedical and nanomedicine application. Pharmaceutics. 2022 Feb;14(3):543. doi: 10.3390/pharmaceutics14030543, PMID 35335920.
41. Nayak D, Shetty MM, Halagali P, Rathnanand M, Gopinathan A, John J. Formulation optimization and evaluation of ibuprofen-loaded menthosomes for transdermal delivery. Int J Pharm. 2024 Nov;665:124671. doi: 10.1016/j.ijpharm.2024.124671, PMID 39245088.
42. Manjushree H, Nayak D, Halagali P, Rathnanand M, Tawale R, Ananthmurthy K. Menthol-based novel ultra-deformable vesicle: formulation optimization and evaluation of an antifungal drug. AAPS PharmSciTech. Jan. 2025;26(1):23. doi: 10.1208/s12249-024-03021-3, PMID 39779535.
43. Gaur PK, Bajpai M, Mishra S, Verma A. Development of ibuprofen nanoliposome for transdermal delivery: physical characterization *in vitro/in vivo* studies and anti-inflammatory activity. Artif Cells Nanomed Biotechnol. 2016 Jan;44(1):370-5. doi: 10.3109/21691401.2014.953631, PMID 25211229.
44. Kar K, Sudheer P. Formulation and evaluation of niosomal drug delivery system of ketoprofen. RGUHS J PharmSci. 2016 Jan;5(4):173-80. doi: 10.5530/rjps.2015.4.7.
45. Ghanbarzadeh S, Arami S. Enhanced transdermal delivery of diclofenac sodium via conventional liposomes, ethosomes and transfersomes. BioMed Res Int. 2013;2013:616810. doi: 10.1155/2013/616810, PMID 23936825.
46. Das J, Debbarma A, Lalhlenmawia H. Formulation and *in vitro* evaluation of poly-(D, L-Lactide-CO-Glycolide) (PLGA) nanoparticles of ellagic acid and its effect on human breast cancer MCF-7 cell line. Int J Curr Pharm Sci. 2021;13(5):56-62. doi: 10.22159/ijcpr.2021v13i5.1887.
47. Egla M, Rajab NA. Sericin-based paclitaxel nanoparticles: preparation and physicochemical evaluation. Iraqi J Pharm Sci. 2025 Feb;33((4SI)):169-78. doi: 10.31351/vol33iss(4SI)pp169-178.
48. Elkomy MH, Eid HM, Elmowafy M, Shalaby K, Zafar A, Abdelgawad MA. Bilosomes as a promising nanoplatform for oral delivery of an alkaloid nutraceutical: improved pharmacokinetic profile and snowballed hypoglycemic effect in diabetic rats. Drug Deliv. 2022 Dec;29(1):2694-704. doi: 10.1080/10717544.2022.2110997, PMID 35975320.
49. Duche G, Sanderson JM. The chemical reactivity of membrane lipids. Chem Rev. 2024;124(6):3284-330. doi: 10.1021/acs.chemrev.3c00608, PMID 38498932.
50. Abdulbaqi IM, Darwis Y, Khan NA, Assi RA, Khan AA. Ethosomal nanocarriers: the impact of constituents and formulation techniques on ethosomal properties *in vivo* studies and clinical trials. Int J Nanomedicine. 2016;11:2279-304. doi: 10.2147/IJN.S105016, PMID 27307730.
51. Park H, Sut TN, Yoon BK, Zhdanov VP, Cho NJ, Jackman JA. Unraveling how cholesterol affects multivalency-induced membrane deformation of sub-100 nm lipid vesicles. Langmuir. 2022 Dec;38(51):15950-9. doi: 10.1021/acs.langmuir.2c02252, PMID 36515977.
52. Mohammed Ali MHM. Preparation and *in vitro* evaluation of transferosome-based gel of meloxicam. Hilla Univ Coll J Med Sci. 2025 May;3(1):28-35. doi: 10.62445/2958-4515.1047.
53. Budai L, Budai M, Fulopne Papay ZE, Vilimi Z, Antal I. Rheological considerations of pharmaceutical formulations: focus on viscoelasticity. Gels. 2023 Jun;9(6):469. doi: 10.3390/gels9060469, PMID 37367140.
54. Malik B, Bekir E. Formulation and *in vitro* /*in vivo* evaluation of silymarin solid dispersion-based topical gel for wound healing. Iraqi J Pharm Sci. 2023;32 Suppl:42-53. doi: 10.31351/vol32issSuppl.pp42-53.
55. Sarhan F, El Gogary R, Yassin M, Soliman M. Penetration enhancer containing vesicles for dermal and transdermal drug delivery a review. Arch Pharm Sci Ain Shams Univ. 2023;7(2):348-75. doi: 10.21608/aps.2023.246357.1141.
56. Watanabe H, Obata Y, Onuki Y, Ishida K, Takayama K. Different effects of l-and d-menthol on the microstructure of ceramide 5/cholesterol/palmitic acid bilayers. Int J Pharm. Dec. 2010;402(1-2):146-52. doi: 10.1016/j.ijpharm.2010.09.038.
57. Chen L, Ma L, Yang S, Wu X, Dai X, Wang S. A multiscale study of the penetration-enhancing mechanism of menthol. J Tradit Chin Med Sci. 2019 Oct;6(4):347-54. doi: 10.1016/j.jtcms.2019.10.001.